RSC Advances

ROYAL SOCIETY OF CHEMISTRY

www.rsc.org/advances

RSC Advances

RSCPublishing

ARTICLE

Catalytic Oxidation of Ascorbic Acid *via* Copper-Polypyridyl Complex Immobilized on Glass

Cite this: DOI: 10.1039/x0xx00000x

Vikram Singh,*[a] Prakash Chandra Mondal,[ab] Megha Chhatwal,[a] Yekkoni Lakshmanan Jeyachandran[c] and Michael Zharnikov*[c]

Received 00th January 2012,
Accepted 00th January 2012

DOI: 10.1039/x0xx00000x

www.rsc.org/

A monolayer of redox-active copper-polypyridyl complexes was prepared on glass and silicon substrates. The monolayer was characterized in detail by a combination of complementary surface analysis techniques. The immobilized complex was utilized for catalytic oxidation of ascorbic acid. The surface bound catalyst was found to be temporally and thermally stable, efficient, as well as partially recyclable. It also showed marked improvement over the performance of the same complex under homogeneous conditions, in terms of the catalytic activity and turnover numbers. Such supported catalyst systems are drawing significant attention as they enable merging the virtues of homogeneous and heterogeneous catalysis.

1. Introduction

Surface assembly of polypyridyl complexes of transition metals by both top-down and bottom-up fabricating methodologies is an active area of research,[1-3] as it presents an opportunity to incisively engineer and combine both molecular and surface attributes, adjusting chemical, optical, structural, magnetic and electrochemical properties of the entire system.[4-8] Besides, this platform has significant potential applicability in logic operations,[9,10] sensing,[11-12] drug delivery,[13] artificial nuclease activity,[14,15] and catalysis.[16] Among these issues, catalysis mediated by supported molecular films is a largely unexplored field. Potentially, a proper immobilization of suitable molecules on a solid support, including nanoparticles (NPs),[17-22] should result in the desired exposure of the receptors or active sites toward the reactants.[23-25] Whereas NP supported catalytic systems have certainly more potential for practical applications, model studies, dealing with the general methodology of the approach, should be better performed on a flat support, which allow better control of the experiments and easier analysis of their results.[26] Generally, molecular assembly on flat surfaces is considered as an excellent platform for studying and finding out mechanistic details of reactions at interfaces.[27] Also, such an assembly can be easily combined with a microfluidic system, which simplifies the experiments.

Homogeneous and heterogeneous catalytic systems frequently face recovery problems and suffer from low yield and limited reusability.[28-30] In contrast, analogous self-assembled monolayer (SAM) based systems offer customized design, ease of recovery and recyclability, in addition to marked stability and superior activity through "acceleration effects" as exemplified by typically large turnover numbers.[31] This has been demonstrated in several experiments in which SAMs containing metallo-ligand complexes were used for catalysis. In particular, functionalized rhodium phosphanes on gold[32] and palladium complexes on silicon[33] were used for catalyzing hydrosilylation of alcohols and aerobic oxidation of benzylic alcohols, respectively. In another example, a palladium surface covered with alkanethiol SAMs showed enhanced regioselectivity towards the reduction of unsaturated epoxides.[34] Further, a Fe-phthalocyanine monolayer on Ag (110) surface has been utilized for oxygen reduction reaction.[35] Significantly, functional SAMs can potentially unite the advantages of homogeneous, heterogeneous, and enzymatic catalysis at a single platform, including heterogenization of the homogeneous catalyst through structural manoeuvres.[16,31,36,37]

A relevant issue in this context is the oxidation of ascorbic acid (Vitamin C, AA) which is a well known biochemical reaction.[38,39] Note that AA is an organic acid soluble in water. It oxidizes to dehydroascorbic acid (DHA) which permeates easily through blood-brain barrier where it quickly reduces back to AA, raising the brain antioxidant level.[40] In its turn, DHA is known to have strong antiviral capability against three different classes of viruses, viz. herpes simplex virus type 1 (HSV-1), influenza virus type A, and poliovirus type 1. Accordingly, the degree of cytotoxicity of the DHA against these viruses has been found to be 10-fold of AA.[41,42] Additionally, DHA was found to inhibit enzymatic activity of IκB kinase, resulting in inhibiting NF-κB activation; thus, potentially playing an important role in decreasing inflammation and perhaps oncogenesis, much like salicylate and aspirin.[43]

In this context, keeping in mind the involvement of DHA in the biochemical processes and prospects of SAM based catalysis in general, we report here a detail study on the oxidation of AA by a supported (glass), siloxane anchored monolayer of custom designed copper complexes (**1**) which have pyridine as a pendant group (see Scheme 1). We took advantage of the flexible molecular design of such complexes that exhibit oxidation-state-dependent geometry variations. To the best of our knowledge, this is the first study of SAM based oxidation of AA, as other notable reports focused mainly on the detection of AA, particularly, on electrode surface[44,45] and nanoparticles,[46,47] utilizing the oxidation/reduction behaviour of AA. Moreover, the present work uses an environmentally benign solvent (water) and a recyclable substrate material (glass), which pertains to green experimental strategy.[48,49] The choice of the glass substrate over other possible supports was intentional, since glass is inexpensive and optically transparent material that allows robust, siloxane-based covalent attachment of the copper complexes. The **1**-based monolayer was well defined as follows from its detailed characterization by X-ray photoelectron spectroscopy (XPS), near edge X-ray absorption fine structure (NEXAFS) spectroscopy, atomic force microscopy (AFM), ellipsometry, and UV-Vis spectroscopy.

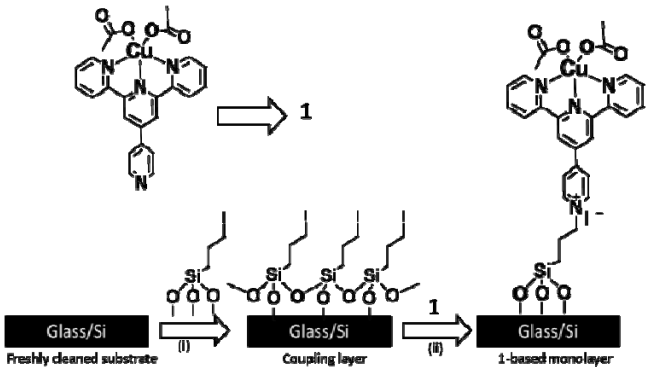

Scheme 1 A schematic representation of fabrication of 1-based monolayer on glass or Si support. (i) immobilization of 3-iodo-*n*-propyl-trimethoxysilane to form a coupling layer. (ii) quaternization of the pendant pyridyl group of 1 to form an 1-based monolayer with the acetate moiety termination.

2. Experimental

2.1 Synthesis of complex 1[50]

Copper acetate monohydrate (0.193g, 0.96 mmol) was dissolved in 10 mL of methanol at room temperature. A boiling methanolic solution of 4'-pyridyl-2,2':6',2''-terpyridine (0.30g, 0.96 mmol) was added dropwise in 30 minutes span time and the solution was stirred for further 2h at 60 ^{o}C. The solution was filtered when hot. The filtrate was cooled to room temperature and slow diffusion of diethyl ether to this solution yielded needle shaped green colour single crystals.

2.2 Fabrication of monolayer of complex 1[51]

The freshly cleaned glass and Si substrates (20 mm × 10 mm × 1 mm) were functionalized with 3-iodo-*n*-propyltrimethoxy-silane under N_2 atmosphere using Glove Box. The substrates were initially treated with a dry *n*-pentane solution of 3-iodo-*n*-propyltrimethoxy-silane (200:1) at room temperature for 30 min under N_2 atmosphere. Then the substrates were thoroughly washed with dry *n*-pentane and sonicated (for 3 min each) with *n*-pentane, followed by washing with dichloromethane (DCM) and 2-propanol to remove any physisorbed materials. The resulting films were dried properly under a stream of N_2 followed by drying in oven at 120 ^{o}C for 15 min. Consequently, the functionalized substrates were placed into 50 mL Teflon-lined autoclave, immersed in dry acetonitrile/toluene solution (3:7, v/v) of complex **1** (0.5 mM), and then kept at 85 ^{o}C for 52 h in a programmed oven. The oven was subsequently cooled to room temperature. The resulting, functionalized substrates were rinsed with acetonitrile and sonicated for 3 min each in acetonitrile, acetone, and 2-propanol to remove physisorbed materials. Finally, the samples were carefully wiped with a wet task wipe and dried under a stream of N_2.

2.3 Preparation of AA solution

A stock solution of 1.0 M of AA was prepared by dissolving 17.6 g of AA in 100 mL DI water (degassed with liquid N_2) and kept in an air tight glass vessel. This solution was further diluted to generate specific solutions having different amounts (concentrations) of AA as required during the experiments.

2.4 UV-Vis spectroscopy

UV-Vis spectra were recorded with JASCO UV-Vis NIR spectrophotometer in a range of 200-600 nm in transmission mode. The samples were placed in 3 mL quartz cuvettes (total capacity) with 1 cm path length. DI water was used for the baseline corrections. The total volume in cuvette was always maintained at 2 mL. As mentioned in the previous section, the sample size, corresponding to the active area of the catalyst, was always kept at 2 × 1 cm^2, at the monolayer coverage of the catalyst-bearing molecules (0.41 nmol per cm^2; see below).

2.5 XPS and NEXAFS spectroscopy

XPS measurements were performed using a Mg Kα X-ray source and a LHS 11 analyzer. The spectra acquisition was carried out in normal emission geometry with an energy resolution of ~0.9 eV. The X-ray source was operated at a power of 260 W and positioned ~1.5 cm away from the samples.

The NEXAFS spectroscopy measurements were performed at the HE-SGM beamline (bending magnet) of the synchrotron storage ring BESSY II. The spectra acquisition was carried out at the C, N, and O K-edges in the partial electron yield mode with retarding voltages of −150, −300, and −350 V, respectively. Linear polarized synchrotron light with a polarization factor of ~91% was used. The energy resolution was ~0.3 eV at the C K-edge and somewhat lower at the N and O K-edges. The incidence angle of the light was varied from 90° (**E**-vector in the surface plane) to 20° (**E**-vector nearly normal to the surface) in steps of 10°-20° to monitor the orientational order of the target films. This approach is based

on the linear dichroism in X-ray absorption, i.e., the strong dependence of the cross-section of the resonant photoexcitation process on the orientation of the electric field vector of the linearly polarized light with respect to the molecular orbital of interest.[52] The raw spectra were normalized to the incident photon flux by division by a spectrum of a clean, freshly sputtered gold sample. Further, the spectra were reduced to the standard form by subtracting a linear pre-edge background and normalizing to the unity edge jump. The photon energy scale was referenced to the most intense π* resonance of highly oriented pyrolytic graphite (HOPG) at 285.38 eV.[53]

2.6 ESI-Mass spectroscopy

Mass spectra of AA and its oxidized products were recorded with THERMO Finnigan LCQ Advantage max ion trap mass spectrometer. For AA, 1 μg/mL solution was prepared in N_2 purged, DI water. For AA oxidation products, 500 μL of solution were directly taken from reaction cuvette.

2.7 FT-IR spectroscopy

FT-IR spectra were recorded with Perkin-Elmer FT-IR spectrometer in a range of 400-4000 cm^{-1} using N_2 purged DI water as medium. DI water was used for the baseline corrections. The samples were prepared in the similar way as in the case of ESI-MS.

3. Results and Discussion

3.1 Monolayer Characterization

UV/Vis measurements on the fabricated monolayer showed that the complexes **1** adhered strongly to the substrate surface as they could not be removed by either the ''scotch tape decohesion'' test or by a stream of critical carbon dioxide (snow-jet).[54] Static aqueous contact angle measurements revealed that this parameter changed from <20° for the freshly cleaned silicon substrate to 67° (± 5°) for the monolayer of **1**, which is reasonable since the latter is apparently more hydrophobic. Semi-contact AFM measurements on the monolayers of **1** grown on Si(100) substrates showed an essentially smooth film surface. The root-mean-square surface roughness, R_q, for these films was ~0.13 nm and peak-to peak roughness, R_y, was ~0.98 nm, for 500 nm x 500 nm scan areas (see Fig. S1 in the Supporting Information).

XPS analysis of the **1**-based monolayer revealed the expected, characteristic emissions from the substrate (SiOx/Si) and the attached molecules. In particular, the Si 2p spectrum exhibited two characteristic doublets at 99.15 and 102.6 eV associated with the bulk Si and SiOx, respectively (Fig. 1a).[55] The relative intensity of the former doublet increased with the increasing sampling depth of XPS, which suggests, as expected, that only the topmost part of the Si substrate was oxidized. The N 1s spectrum of the monolayer exhibited two emissions at 399.4 and 402.0 eV related to the pyridine (N) and pyridinium (N+) nitrogen atoms, respectively (Fig. 1b).[56,57] The intensity ratio of these emissions, viz. 2.8, correlates well with the chemical compositions of the immobilized complexes (the N/N+ ratio for 1 is 3). The Cu 2p spectrum of the monolayer exhibited a pronounced Cu 2p3/2,1/2 doublet at 932.1 and 951.9 eV (Fig. 1c), highlighting the expected presence of copper.[58,59]

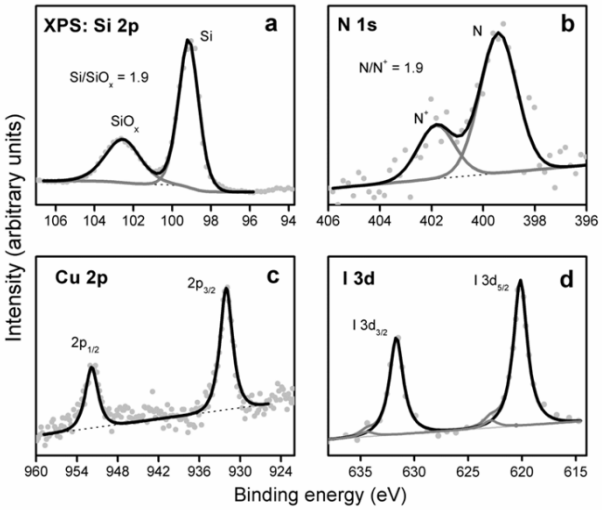

Fig. 1 Si 2p (a), N 1s (b), Cu 2p (c), and I 3d (d) XP spectra of 1-based monolayer on Si(100) substrate. The filled circles represent the experimental data; the black solid lines are the respective envelopes or fits. The N 1s spectrum is decomposed into two components related to coordinated N-atoms and pyridinium N^+. The I 3d spectrum is decomposed into two doublets related to ionic I atom (black line) and covalently bonded I atom (grey line).

Finally, the I 3d XP spectrum of the **1**-based monolayer in Fig. 1d was dominated by the $3d_{5/2,3/2}$ doublet at 620.13 eV (I $3d_{5/2}$) which can be assigned to ionic iodine,[60,61] in agreement with the expected composition of the monolayer (Fig. 1d). This doublet was accompanied by a much weaker one at 622.93 eV (I $3d_{5/2}$) which can be attributed to methylene iodide ($-CH_2I$). The intensity ratio of the anionic and methylene doublets was found to be 10:1, which suggests a low content of the methylene iodide and, consequently, a uniform character of the monolayer.

Complementary to the XPS data, NEXAFS spectra of the **1**-based monolayer were recorded at the C, N, and O K-edges. The incidence angle of X-rays was varied to monitor possible orientational order within the monolayer. The C K-edge spectra showed a characteristic, double-peak resonance at ~285 eV typical of pyridine in the given specific terpyridine arrangement (Fig. 2a).[62] This pre-edge feature consists presumably of three individual π* type resonances which are partly merged together.[63,64] The complex character of this feature as compared to the single π_1* resonance of benzene at 285.0 eV[56] is mostly related to the different C 1s core level binding energies for the carbon atoms in the *ortho* positions (C=N) and those in the *meta* and *para* positions (C=C) of the pyridine rings.[63,64] In addition, there are two further, distinct resonances at ~287.5 and ~288.6 eV, overlapping with the absorption edge. The former resonance is presumably related to the pyridine rings,

while the latter resonance can be associated with the excitation in the π^* orbital of the terminal acetate groups.[65] The N K-edge spectra are dominated by a single π^* resonance at ~399.6 eV assigned to the excitation of the N1s core level electron into the LUMO orbital of the pyridine rings (Fig. 2b).[64] The O K-edge spectra are dominated by an intense π^* resonances at ~537 eV accompanied by several σ^* resonances at higher photon energies (see Fig. S2 in the Supporting Information).[65] The NEXAFS spectra at both C and K edge did not exhibit noticeable changes in the intensity of the characteristic absorption resonances upon the variation of the incidence angle of X-rays (see the respective difference spectra as Fig. S3 in the Supporting Information). This means that the complexes 1 did not exhibit a preferable orientation in the monolayer.[66]

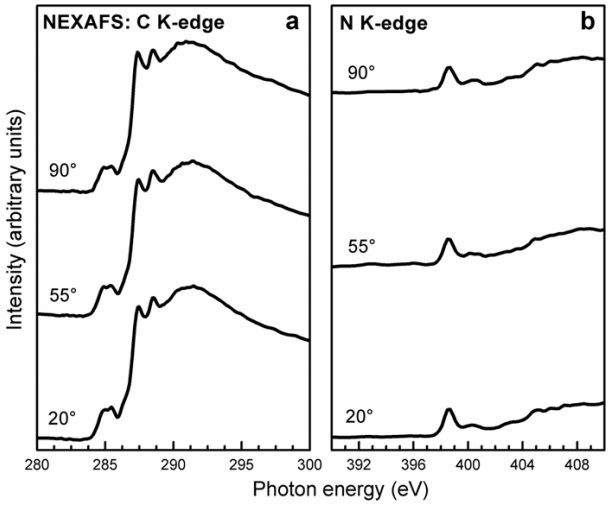

Fig. 2 C K-edge (a) and N K-edge (b) NEXAFS spectra of 1-based monolayer on Si(100) substrate. The spectra were acquired at X-ray incident angles of 90°, 55°, and 20°. There are no noticeable changes in the intensity of the characteristic resonances upon the variation of the acquisition geometry.

The UV-Vis absorbance spectrum of the **1**-based monolayer on glass showed a characteristic ligand-to-metal charge transfer band at λ_{max}= 356 nm. This spectrum was similar to the analogous spectrum of **1** in solution but had a red shift of the absorption band position by ~8 nm (see Fig. S4 in the Supporting Information).[67] Increasing the reaction time from 52 to 64 hours did not affect the optical absorption or the position of the band, indicating the completeness of the monolayer formation within the given preparation time. In contrast, shortening the reaction time from 52 to 20 hours resulted in decrease in optical absorption of the **1**-based monolayer by a factor of ~ 4. Interestingly, the estimated volume-per-molecule for **1** on the glass surface, V = 0.4–0.6 nm^3, corresponds approximately to the respective value for complex **1** in the unit cell of the crystal structure, V = 1.1 nm^3 with two molecules in the unit cell as observed in our previous work.[68] The ellipsometry derived thickness of the **1**-based monolayer was ~1.4 ± 0.3 nm, and the refractive index, *n*, at λ = 550 nm (non-absorbing region) was 1.66. Note that the above thickness value is in good agreement with the XPS derived one (~1.2 nm). The molecular density in the monolayer was estimated at ~40 $Å^2$ per molecule or 0.41 nmol per cm^2 by UV-Vis spectroscopy; the above values are reasonable for such species.[68,69]

3.2 Catalytic activity of the monolayer

1-based catalytic oxidation of AA was monitored optically using an off-the-shelf UV-Vis NIR spectrophotometer; the measurements were performed in a range of 200-600 nm, in transmission mode. At first, a reference UV-Vis spectrum of 300 nmol of AA dissolved in 2 mL of DI water (corresponding to 150 μM concentration) was recorded; this spectrum exhibited an intense absorption band with λ_{max} = 264 nm. Then, the same amount of the fresh AA solution was brought in contact with the **1**-based monolayer on a 2×1 cm^2 support, and the **1**-catalysed reaction was monitored by UV-Vis spectroscopy. The spectra were acquired subsequently for about 4 hours with no stirring and at room temperature. It was then observed that the intensity of the characteristic absorbance band, representative of the concentration of the AA solution, decreased gradually with the time until it disappeared almost completely after 4 hours (Fig. 3). When the reaction was performed for a longer time, an absorption band of low intensity at λ_{max} = 288 nm appeared, implying that species other than AA were present. Most likely these are oxidation products of AA such as DHA (oxidation products of AA absorb very little in the given spectral region).[70,71] Within this process, neutral form of AA, at first, dissociated reversibly to its monoionic form (ascorbate anion), which was a slow step. Subsequently, ascorbate anion started a series of reaction at liquid-solid interface by coordinating to Cu(II), which eventually led to the AA oxidation.[72,73]

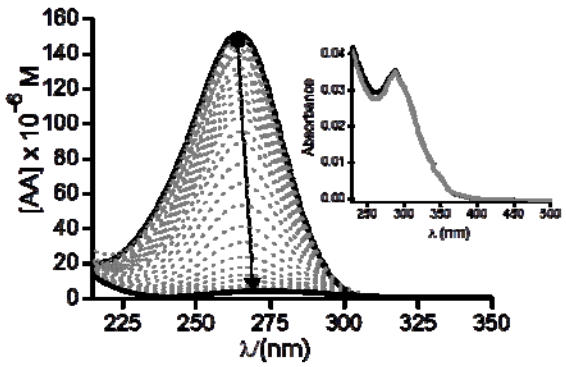

Fig. 3 Subsequently acquired UV-Vis absorption spectra of AA solution (150 μM) exposed to the 1-based monolayer from the beginning of the reaction (t = 0; top curve; highlighted by thick black line) to t = ~ 4 hours (bottom curve; highlighted by thick black line). Inset shows the appearance of a new band of very low intensity with λ_{max} = 288 nm upon a prolonged exposure (t > 4 hours). The oxidation products of AA, viz. DHA and DKG do not exhibit intense absorption bands in the given spectral range.

To verify the fact that the observed change of the UV-Vis spectra was primarily due to the monolayer based oxidation of AA and not due to water or glass slide, control measurements with no glass slide and a blank glass slide (2x1 cm^2) were performed at the same conditions as the experiments with the

functionalized slide. No significant changes in the UV-Vis spectra were observed, which suggests that the changes occurring in the case of the **1**-based monolayer (Fig. 3) can be indeed attributed to the oxidation-reduction reaction between the Cu(II) centre of the monolayer and AA. To stress the role of this centre, we added copper metal (Cu (0)) to AA solution for ~4 hours in another set of control experiments. Similar to the case of the blank glass slide, no significant changes in the UV-Vis spectra were observed, which imply that Cu (II) oxidation state is necessary for carrying out the reaction.

To make a quantitative comparison, a plot of the AA conversion in percent with respect to time (in seconds) was made (Fig. 4). According to this plot there is just a ~4-6 % decline in the absorbance of the AA solution in the cases of the blank glass slide and water without glass slide, while the conversion for the **1**-based monolayer approached ~97% after 4 hours. The plot of –log [AA] *vs.* time (in seconds) gives a straight line, suggesting a first order reaction for the **1**-mediated oxidation of AA. A linear fit of the experimental data according to the first order reaction equation

$$[AA] = [AA]_{initial} \times \exp(-k_1 T) \qquad (1)$$

gives a rate constant, k_1, of ~2.82×10^{-4} s^{-1}.

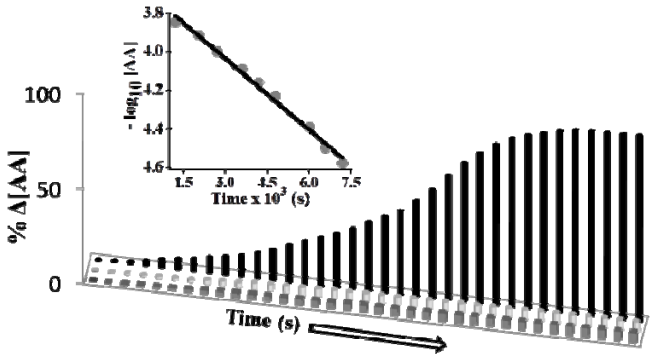

Fig. 4 Change in the AA concentration upon exposure of its fresh solution in water to 1-based monolayer (black bars) or to blank glass slide (light grey bars) or just keeping it (grey bars) for ~4 hours. The change in the AA concentration was only ~4-5% in two latter cases but amounted ~98% at the exposure to the monolayer. Inset: semi-logarithmic plot of the AA concentration as a function of time, along with the respective linear fit (R^2 = 0.99) suggesting the first order kinetics for the 1-catalyzed oxidation of AA.

In further experiments we varied the amount of AA participating in the reaction, dissolving 60 to 2000 nmol of AA in 2 mL of DI water, which corresponds to a concentration range of 30 to 1000 μM and to a substrate to catalyst ratio (S/C) of 40 to 650 for the given **1**-functionalized slide area (2 cm^2). The resulting solutions were subjected individually to the **1**-based oxidation for 4 hours. As expected, small amounts of AA (60-300 nmol) got oxidised almost completely, resulting in high turnover numbers approaching the S/C ratios (see Table 1). For the larger amount (2000 nmol), the oxidation was not complete and, consequently, the turnover number was significantly smaller than the S/C ratio. The respective experiments were repeated two more times with different glass slides of the **1**-based monolayer of the same area; the extent of the AA conversion was essentially the same, within an error of ±2%, which justifies the results. In addition to the above study, we explored the impact of much higher concentrations of AA on conversion efficiency and turnover numbers (see Table 1). In particular, 100 μmol of AA dissolved in 2 mL of DI water (corresponding to 50 mmol concentration) with a S/C of 243900 were exposed to the **1**-based monolayer (2×1 cm^2). As expected, we observed that in the time-frame of ~4 hours, there was only 13% conversion but this still provides a high turnover number of 31700. In addition, we also compared the catalytic activity of the **1**-based monolayer with Cu(II) complex in solution (homogeneous catalysis) ($MeOH/H_2O$ mixture, 1:1 (v/v)). The homogeneous catalysis demonstrated an inferior efficiency with low conversion percents at various S/C ratios under the similar conditions. For instance, 60 nmol of AA provided only ~25% conversion (TON = 37), which is significantly lower than ~98% (TON = 147) as observed for the monolayer based catalysis. Similar differences in reaction yield were also noticed for the higher amounts of AA at the same S/C ratios (see Table 1). The observed lower yields for the homogeneous catalysis are in agreement with the previously reported results by Fernandes et al.[31], Sawamura et al.[32,33] and Benitz et al.[26] and can be tentatively explained by partial aggregation of the catalyst molecules in solution, leading to their deactivation. In contrast, according to Belser et al.,[17] in the case of heterogeneous catalysis, aggregation of the catalyst molecules is rather unlikely due to the separation of the catalytic centers upon the immobilization, which improve reaction yields. In addition, immobilization of the catalyst allows favorable orientation of these catalytic centers, which is suggested to be a further factor in improving reaction yields.[18,27] Our results, therefore, can be tentatively explained along these lines.

Table 1 Parameters of the catalytic reaction mediated by the 1-based monolayer (2 cm^2, 0.41 nmol cm^{-2}) for different concentrations of AA in N_2 purged, DI water.

Entry	[AA]/nmol	S/C	Conversion %[a]	TON[a]
1	60	150	98(25)[b]	147(37)
2	100	240	95(28)	235(67)
3	300	730	92(26)	670(189)
4	2000	4880	51(15)	2490(732)
5	10000	24390	26(5)	6340(1219)
6	100000	243900	13(4)	31700(9756)

[a] After 4 h of reaction as determined by UV-Vis spectroscopy. [b] Conversion % and TONs in the brackets correspond to the reaction with the homogeneous **1**-based catalytic system (solution study) under the similar conditions.

In another set of experiments, we tested the lifetime and reusability of the **1**-based monolayer catalyst. For this purpose, the monolayer was exposed four times, in a successive fashion, to either 60, 100, or 300 nmol of AA dissolved in 2 mL of DI water. Each exposure (run) took 4 h and the amount of the residual AA was monitored optically. After each exposure, the catalyst was *regenerated* by keeping it in air/O_2 for ~5 minutes. Independent of the amount of AA, we could observe a high conversion yield in the first run, but the catalytic activity reduced noticeably with each subsequent run. The extent of the reduction was larger with increasing amount of AA in the solution as shown in Fig. 5. Such a reduction in the catalytic ability could be related to subtle equilibrium between the catalytic transformations and successive deactivation of the catalyst.

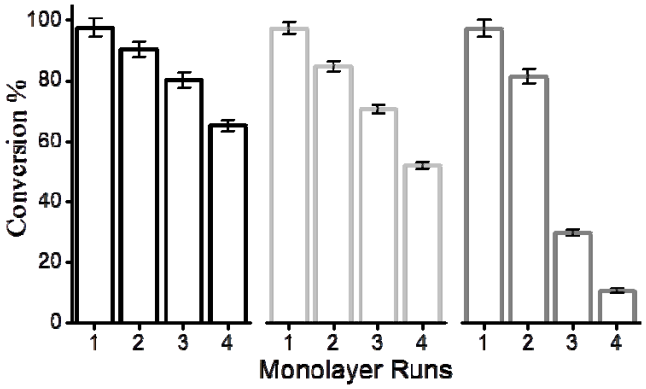

Fig. 5 A reusability test for the 1-based monolayer catalyst. The monolayer was exposed four times, in a successive fashion, to either 60 nmol (left panel), 100 nmol (middle panel) or 300 nmol (right panel) of AA dissolved in 2 mL of DI water. Each run took 4 h. The catalyst was reset with air/O_2 between the runs. After the fourth run, conversion dropped to ~65 % and ~12 % for 60 and 300 nmol of AA, respectively.

To rationalise the above observations, UV-Vis spectra of the monolayer were recorded after the regeneration and it was found that the monolayer absorbance declined per run. Moreover, evaluation of the surface density of **1** from the UV-Vis data, on the basis of the characteristic ligand band at λ_{max}= 278 nm, revealed that this density decreased faster after each run for higher concentrations of AA. For instance, whereas the surface density of the pristine monolayer was ~0.41 nmol per cm^2, it dropped down to 0.28 nmol per cm^2 after four runs of exposure to 300 nmol of AA (Fig. 6a). This plunge in the surface density can be presumably attributed to loss of acetate ions during the reaction with concomitant geometry change around the metal centre or to possible contamination of the surface.[68] Note that the leaching of copper from the monolayer could be possibly neglected as the rationale for the observed drop in the catalytic activity as the LMCT bands at λ_{max}= ~ 354 nm exhibited only a slight decrease in its absorbance. To substantiate our claim, we kept the monolayer in saturated sodium acetate solution (O_2 saturated) for ~10 minutes after each run (160 nmol AA) performed this time for ~2 hours and it was found that the conversion decreased to ~31% after four runs (Fig. 6c), which is a more substantial drop as compared to the air/O_2 regeneration of the monolayer (Fig. 5). This puts into perspective the supposed scenario of acetate ions getting drained into the solution. On this basis, a probable mechanism is proposed for the AA oxidation (see also Fig. S5 in the Electronic Supplementary Information), where AA forms ascorbate anion which acts on Cu(II) resulting in release of acetate ion. Electron transfer from ascorbate moiety to Cu(II) reduces it to Cu(I) and oxidizes AA to DHA. During regeneration of the catalyst, **1**-based monolayer is kept in saturated solution of sodium acetate (O_2 saturated), where O_2 oxidizes Cu(I) back to Cu(II). Presence of acetate ions probably favours the regeneration of the original catalyst.[68,72,73]

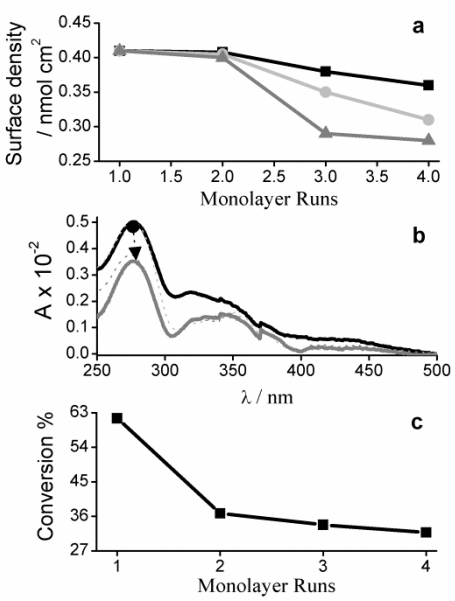

Fig. 6 (a) Surface density of the 1-based monolayer exposed four times, in successive fashion, to 60 (black line), 100 (light grey line), or 300 (grey line) nmol of AA, measured after each run by UV-Vis spectroscopy. (b) Representative UV-Vis spectra of the 1-based monolayer after the end of 4th run for the case of 60 nmol AA exposure. c) The change in the conversion of the oxidation reaction in the case of the regeneration with O_2 saturated solution of NaOAc. The duration of the AA exposure (160 nmol) in each run was 2 hours.

3.3 Product analysis

A qualitative analysis of the oxidation products of AA was performed by a combination of electrospray ionization mass spectroscopy (ESI-MS, +ve mode) and FT-IR spectroscopy. The ESI-MS analysis of AA and its oxidation products in N_2 purged, DI water validated the reasoning and arguments made in the above sections. AA and its oxidation products can form sodium adducts in ESI-MS and this is what we have primarily observed. Interestingly, in the mass spectrum of AA (see Fig. S6 in the Supporting Information),[74] AA appeared in dimeric form as the most abundant ion at *m/z* = 375 $(M + Na)^+$ while the respective monomer appeared at *m/z* = 199 $(M + Na)^+$ with lower intensity, accompanied by even weaker peak at *m/z* = 198

and a peak at *m/z* = 177 assigned to AA without sodium adduct $(M + H)^+$. The peak at m/z = 198 could be possibly attributed to a keto form of AA, formed due to the loss of H^+ ion from one of the enolic hydroxyls. It appears that the keto form is less stable than the enolic form of AA as the intensity at *m/z* = 199 is higher than at m/z = 198. In the mass spectrum of the same solution after the AA oxidation *via* **1**-based monolayer, new peaks at *m/z* = 192, 214, and 215 were observed (see Fig. S7 in the Supporting Information); they could be attributed to hydrated bicyclic hemiketal of DHA or DKG (M, $M + Na)^+$, respectively.[75-77] In addition, low intense peaks were observed at *m/z* of 349 $(M + H)^+$ and 365 and ascribed to the formation of dimeric DHA and hydrated dimeric DHA, respectively. Expectedly, it was observed that the peaks at *m/z* = 375 and *m/z* = 199 disappeared completely, emphasizing the fact that AA has been oxidised. Thus, the ESI-MS results clearly indicate that the catalytic system of the **1**-based monolayer effectively oxidizes AA to DHA and DKG in their hydrated, dimeric or hemiketal forms. Significantly, ESI-MS did not show any peak corresponding to leaching of **1** or large fragments from the monolayer, which means that the analyzed solutions were free from catalyst-related contamination.

Complimentary to the ESI-MS studies, FT-IR spectroscopy was used to investigate the interactions between the involved species and changes in the chemical compositions, that is, from the reactant to product. FT-IR spectra of AA and its oxidation products taken from the same solution (AA in N_2 purged, DI water) before and after the catalytic process, respectively, reveal the expected picture.[79-81] In the FT-IR spectra of AA in Fig. 7a, peaks in a region of 3000 - 3500 cm^{-1} could be tentatively designated to the hydroxyl groups; peaks at 1669 and 1327 cm^{-1} correspond to carbon-carbon double bond and enol-hydroxyl, respectively, and match with the reported FT-IR spectra of AA.[79-81] In the FT-IR spectrum of the oxidation products in Fig. 7b, peaks at 3320, 1718, 1655, and 1636 cm^{-1} are tentatively assigned to hydroxyl, oxidated ester carbonyl groups, and conjugated carbonyl groups corresponding to DHA and DKG, respectively. Further peaks at 1266 and 1029 cm^{-1} are attributed to the carbon-oxygen stretching of the acid and ether groups of DHA.

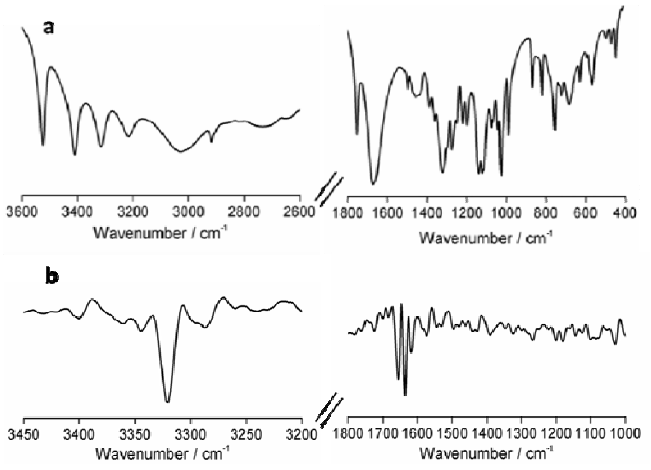

Fig. 7 (a) Transmission FT-IR spectrum of AA in N_2 purged, DI water; the spectrum show characteristic vibrations in a region of 400-3600 cm^{-1}. (b) Transmission FT-IR spectrum of the same solution after the AA oxidation catalysis. See text for details. The units of the Y-axis are % transmission.

4. Conclusions

Monolayer based catalytic oxidation of AA was carried out as a model reaction to study the performance and behavior of a well-defined, supported catalytic system. It was shown that the activity of the monolayer catalyst is noticeably higher as compared to its homogeneous counterpart, which can be tentatively attributed to the ordering and favorable orientation of the molecules upon immobilization.[26, 82, 83] The effect of AA concentration on the activity of the monolayer catalyst was studied in detail and its reusability was ascertained. Also, the products of the catalytic reaction were analyzed. The latter experiments relied on the easy characterization of the reaction products, which was possible in the given case since the monolayer catalyst was easy to remove from the reaction mixture by facile physical transfer.

The above results provide a representative example for the usefulness of monomolecular catalytic assemblies on a solid support. There are, however, still a variety of open questions such as the structure-property relationship in these systems, better reusability, etc. One can also look forward to the possibility to design multi-component monolayers of catalytically active molecules which, due to a synergy effect, could possibly exhibit enhanced catalytic activity compared to the individual species.

Acknowledgements

This work was financially supported by the Department of Science and Technology (SR/S1/IC-19/2009), New Delhi, and the University Grants Commission (F-37-407/2009(SR)), New Delhi. VS thanks UGC for the senior research fellowship. PCM thanks CSIR for senior research fellowship. MC thanks DAE-BRNS for research fellowship. MZ thanks Ch. Wöll and A. Nefedov (KIT) for the technical cooperation at BESSY II and the BESSY II staff for the assistance during the experiments.

Notes and references

[a] *Department of Chemistry, University of Delhi, Delhi-110007, India E-mail: vikram.singh19@yahoo.co.in*
[b] *Department of Chemical Physics, Weizmann Institute of Science, Rehovot-7610001, Israel*
[c] *Applied Physical Chemistry, University of Heidelberg, Im Neuenheimer Feld 253, 69120 Heidelberg, Germany*
E-mail: Michael.Zharnikov@urz.uni-heidelberg.de
†Dedicated to Late Dr. Tarkeshwar Gupta; Electronic Supplementary Information (ESI) available: See DOI: 10.1039/b000000x/

1 A. Ulman, *Chem. Rev.*, 1996, **96**, 1533-1554.
2 J. V. Barth, G. Constantini, K. Kern, *Nature*, 2005, **437**, 671-679.

3 L. Motiei, M. Altman, T. Gupta, F. Lupo, A. Gulino, G., Evmenenko, P. Dutta, M. E. Van der Boom, *J. Am. Chem. Soc.*, 2008, **130**, 8913-8915.
4 T. Gupta, P. C. Mondal, A. Kumar, Y. L. Jeyachandran, M. Zharnikov, *Adv. Func. Mater.*, 2013, **23**, 4227-4235.
5 E. Coronado, P. Gavina, S. Tatay, *Chem. Soc. Rev*,. 2009, **38**, 1674-1689.
6 G. de Ruiter, M. Lahav, G. Evmememko, P. Dutta, D. A. Cristaldi, A. Gulino, M. E. van der Boom, *J. Am. Chem. Soc.*, 2013, **135**, 16533-16544.
7 G. de Ruiter, M. Lahav, H. Keisar, M. E. van der Boom, *Angew. Chem.*, 2013, **52**, 704-709.
8 V. Ferri, M. Elbing, G. Pace, M. D. Dickey, M. Zharnikov, P. Samori, M. Mayor, M. A. Rampi, *Angew. Chem.*, 2008, **120**, 3455-3457.
9 A. P. de Silva, *Nature*, 2008, **454**, 417-418.
10 G. de Ruiter, M. E. Van der Boom, *Acc. Chem. Res.*, 2011, **44**, 563-573.
11 L. Ding, Y. Fang, *Chem. Soc. Rev.*, 2010, **39**, 4258-4273.
12 T. Gupta, M. E. Van der Boom, *J. Am. Chem. Soc.*, 2006, **128**, 8400-8401.
13 V. Singh, M. Zharnikov, A. Gulino, T. Gupta, *J. Mater. Chem.*, 2011, **21**, 10602-10618.
14 N. Higashi, T. Inoue, M. Niwa, *Chem. Commun.*, 1997, 1507-1508.
15 S. Sortino, S. Petralia, G. G. Condorelli, S. Conoci, G. Condorelli, *Lnagmuir*, 2003, 536-539.
16 A. K. Kakkar, *Chem. Rev*,. 2002, **102**, 3579-3588.
17 T. Belser, M. Stohr, A.Pfaltz, *J. Am. Chem. Soc.*, 2005, **127**, 8720-8731.
18 M. Bartz, J. Kuther, R. Seshadri, W. Tremel, *Angew. Chem. Int. Ed.*, 1998, **37**, 2466-2468.
19 N. E. Leadbeater, M. Marco, *Chem. Rev.*, 2002, **102**, 3217-3274.
20 C. E. Song, S. Lee, *Chem. Rev.*, 2002, **102**, 3495-3524.
21 P. McMorn, G. H. Hutchins, *Chem. Soc. Rev.*, 2004, **33**, 108-122.
22 B. S. Rana, S. L. Jain, B. Singh, A. Bhaumik, B. Sain, A. K. Sinha, *Dalton Trans.*, 2010, **39**, 7760-7767.
23 M. Kim, J. N. Hohman, Y. Cao, K. N. Houk, H. Ma, A. K. Y. Jen, P. S. Weiss, *Science*, 2011, **331**, 1312-1315.
24 S.-S. Li, B. H. Northrop, Q.-H.Yuan, L.-J. Wan, P. J. Stang, *Acc. Chem. Res.*, 2009, **42**, 249-259.
25 L.-J. Wan, *Acc. Chem. Res.*, 2006, **39**, 334-342.
26 I. O. Benitez, B. Bujoli, L. J. Camus, C. M. Lee, F. Odobel, D. R. Talham, D. R., *J. Am. Chem. Soc.*, 2002, **124**, 4363-4370.
27 V. Chechik, R. M. Crooks, C. J. M. Stirling, *Adv. Mater.*, 2000, **16**, 1161-1171.
28 G. W. Parshall, D.Ittel, *Homogeneous Catalysis*, Wiley: New York, 1992.
29 L. S. Hegedus, *J. Orgmet. Chem.*, 1992, **422**, 301-681.
30 D. J. C.–H. Hamilton, R. P. Tooze, *Catalysis Separation, Recovery and Recycling, Catalysis by metal complexes*, Springer, 2006, **30**, 1.
31 A. Fernandes, P. Hensenne, B. Mathy, W. Guo, B. Nysten, A. M. Jonas, O. Riant, *Chem. Eur. J.*, 2012, **18**, 788-792.
32 K. Hara, R. Akiyama, S. Takakusagi, K. Uosaki, T. Yoshino, H. Kagi, M. Sawamura, M., *Angew. Chem. Int. Ed.*, 2008, **47**, 5627-5630.
33 K. Hara, S. Tayama, H. Kano, T. Masuda, S.Takakusagi, T. Kondo, K. Uosaki, M. Sawamura,*Chem. Commun.*, 2007, 4280-4282.
34 T. S. Marshall, M. O'Brien, B. Oetter, A. Corpuz, R. M. Richards, D. K. Schwartz, J. W. Medlin, *Nat. Mater.*, 2010, **9**, 853-858.
35 F. Sedona, M. D. Marino, D. Forrer, A. Vittadini, M. Casarin, A. Cossaro, L. Floreano, A. Verdini, M.Sambi, *Nat. Mater.*, 2012, **11**, 970-977.
36 a) F. R. Hartley, *Supported Metal Complexes, A New Generation of Catalysts;* D. Reidel Publishing*:* Dordrecht, Netherlands, 1985.
37 J. M. Basset, B. C. Gates, J.–P. Candy, A. Choplin, M. Leconte, F. Quignard, C. Santini, *Surface Organometallic Chemistry: Molecular Approaches to Surface Catalysis*; Eds.; Kluwer: Dordrecht, Netherlands, 1988.
38 S. Englard, S. Seifter, *Annual Rev. Nutr.*, 1986, **6**, 365-406.
39 A. Hacisevki,*J. Fac. Pharm. Ankara*, 2009, **38**, 233-255.
40 J. Huang, D. B. Agus, C. J. Winfree, S. Kiss, W. J. Mack, R. A. Mctaggart, T. F. Choudhari, L. J. Kim, J. Mocco, D. J. Pinsky, W. D. Fox, R. J. Israel, T. A. Boyd, D. W. Golde, E. S. Connoly, Jr., *Proc. Nat. Am. Soc.*, 2001, **98**, 11720-11724.
41 A. Furuya, M. Uozaki, H. Yamasaki, T. Arakawa, M. Arita, A. H. Koyama, *Intl. J. Mol. Med.*, 2008, **22**, 541-545
42 M. Uozaki, K. Ikeda, K.Tsujimoto, M. Nishide, H. Yamasaki, B. Khamsri, A. H. Koyama, *Exp. Thera. Med.*, 2010, **1**, 983-986.
43 J. M. Carcamo, A.Pedraza, O.–B. Ojeda, B. Zhang, R. Sanchez, D. W. Golde, *Mol. Cell. Biol.*, 2004, **24**, 6645-6652.
44 S. Cosnier, M. Holzinger, *Chem. Soc. Rev.*, 2011, **40**, 2146-2156.
45 S. A. Kumar, P.–H. Lo, S.–M. Chen, *Biosens. Bioelectron.*, 2008, **24**, 518-523
46 S. S. Kumar, K. Kwak, D. Lee, *Anal. Chem.*, 2011, **83**, 3244-3247.
47 Y. Zhang, B. Li, C. Xu, *Analyst*, 2010, **135**, 1579-1584.
48 J. M. De Simone, *Science*, 2002, **297**, 799-803.
49 P. T. Anastas, C.–J. Li, *Handbook of Green Chemistry, Green Solvents, Reactions in water* 2013, **5**.
50 W.–J. Shi, L. Hou, D. Li, Y.–G. Yin, *Inorg. Chim.Acta*, 2007, **360**, 588-598.
51 P. C. Mondal, J. Y. Lakshmanan, H. Himoudi, M. Zharnikov, T. Gupta, *J. Phys. Chem. C*, 2011, **115**, 16398-16404.
52 J. Stöhr, *NEXAFS Spectroscopy*; Springer Series in Surface Science 25; Springer-Verlag: Berlin, 1992.
53 P. E. Batson, *Phys. Rev. B*, 1993, **48**, 2608-2610.
54 B. Y. Chow, D. W. Mosley, J. M. Jacobson, *Langmuir*, 2005, **21**, 4782-4785.
55 N. Koshizaki, H. Umehara, T. Oyama, *Thin Solid Films*, 1998, **325**, 130-136.
56 W. J. Gammon, O. Kraft, A. C. Reilly, B. C. Holloway, *Carbon*, 2003, **41**, 1917-19623.
57 M. Boterashvili, T. Shirman, S. R. Cohen, G. Evmenenko, P. Dutta, P. Milko, G. Leitus, M. Lahav, M. E. van der Boom, *Chem. Commun.*, 2013, **49**, 3531-3533.
58 P. E. Laibinis, G. M. Whitesides, *J. Am. Chem. Soc.*, 1992, **114**, 9022-9028.
59 S. Carniato, G. Dufour, Y. Luo, H. Argen, *Phys. Rev. B*, 2002, **66**, 045105-1 to 045105-12.
60 D. R. Blasini, R. J. Tremont, N. Batina, I. Gonzalez, C. R. Cabrera, *J. Electroanal. Chem.*, 2003, **540**, 45-52.

61 W. H. Fang, D. X. Yong, W. Jing, G. X. Fa, X. G. Mei, S, Z. Jin, L. Y. Fang, Z. Y. Linag, *Acta Phys. – Chim. Sin.*, 2004, **20**, 673-675.

62 J. A. Horsley, J. Stohr, A. P. Hitchcock, D. C. Newbury, A. L. Johnson, F. Sette, *J. Chem. Phys.*, 1985, **83**, 6099-6107.

63 C. Kolczewski, R. Puttner, O. Plashkevych, H. Agren, V. Staemmler, M. Martins, G. Snell, A. S. Schlachter, M. Sant'Anna, G. Kaindl, L. G. M. Pettersson, *J. Chem. Phys.*, 2001, **115**, 6426-6437.

64 H. Hamoudi, K. Döring, F. Chesneau, H. Lang, M. Zharnikov, *J. Phys. Chem. C*, 2012, **116**, 861–870.

65 N. T. Samuel, C.–Y. Lee, L. J. Gamble, D. A. Fischer, D. G. Castner, *J. Electr. Spect. Rel. Phen.*, 2006, **152**, 134-142.

66 S. Richter, J. Poppnberg, C. H.–H. Traulsen, E. Darlatt, A. Sokolowski, D. Sattler, W. E. S. Unger, C. A. Schalley, *J. Am. Chem. Soc.*, 2012, **134**, 16289-16297.

67 M. E. van der Boom, A. G. Richter, J. E. Malinsky, P. A. Lee, N. R. Armstrong, P. Dutta; T. J. Marks, *Chem. Mater.*, 2001, **13**, 15-17.

68 V. Singh, P. C. Mondal, J. Y. Lakhsmanan, M. Zharnikov, T. Gupta, *Analyst*, 2012, **137**, 3216-3219.

69 T. Gupta, M. Altman, A. D. Shukla, D. Freeman, G. Leitus, M. E. van der Boom, *Chem. Mater.*, 2006, **18**, 1379-1382.

70 D. T. Sawyer, G. Chiericato, Jr., T. Tsuchiya, *J. Am. Chem. Soc.*, 1982, **104**, 6273-6278.

71 M. K. Shukla, P. C. Mishra, *J. Mol. Struct.*, 1996, **377**, 247-259.

72 M. M. Khan, A. E. Martell, *J. Am. Chem. Soc.*, 1967, **89**, 4176-4185.

73 M. M. Khan, A. E. Martell, *J. Am. Chem. Soc.*, 1967, **89**, 7104-7111.

74 J. C. Deutsch, *Methods Enzymol.*, 1997, **279**, 13-24.

75 J. C. Deutsch, *Anal. Biochem.*, 1998, **255**, 1-7.

76 J. C. Deutsch, *Anal.Biochem.*, 1998, **265**, 238-245.

77 J. C. Deutsch, *J. Chromato. A*, 2000, **881**, 299-307.

78 D. Williams, L. H. Rogers, *J. Am. Chem. Soc.*, 1937, **59**, 1422-1423.

79 C. Y. Panicker, H. T. Varghese, D. Philip, *Spectrochim. Acta Part A*, 2006, **65**, 802-804.

80 J. Xiong, Y. Wang, Q.Xue, X. Wu, *Green Chem.*, 2011, **13**, 900-904.

81 V. M. Dhavale, S. Kurungot, *J. Phys. Chem. C*, 2012, **116**, 7318-7326.

82 K. Tollner, R. Popovitz-Biro, M. Lahav, D. Milstein, *Science*, 1997, **278**, 2100–2102.

83 A. Pasc-Banu, C. Sugisaki, T. Gharsa, J.-D. Marty, I. Gascon, G Pozzi, S. Quici, I. Rico-Lattes, C. Mingotaud, *Angew. Chem.*, 2004, **116**, 6300–6303.